

# Combined Scanning Electrochemical/Optical Microscopy with Shear Force and Current Feedback

Youngmi Lee, Zhifeng Ding, and Allen J. Bard\*

Department of Chemistry and Biochemistry, University of Texas at Austin, Austin, Texas 78712

**A technique that combines scanning electrochemical microscopy (SECM) and scanning optical microscopy (OM) was developed. Simultaneous scanning electrochemical/optical microscopy (SECM/OM) was performed by a special probe tip, which consists of an optical fiber core for light passage, surrounded by a gold ring electrode, and an outermost electrophoretic insulating sheath, with the tip attached to a tuning fork. To regulate the tip–substrate distance, either the shear force or the SECM tip current was employed as the feedback signal. The application of a quartz crystal tuning fork (32.768 kHz) for sensing shear force allowed simultaneous topographic, along with SECM and optical imaging in a constant-force mode. The capability of this technique was confirmed by obtaining simultaneously, for the first time, topographic, electrochemical, and optical images of an interdigitated array electrode. Current feedback from SECM also provided simultaneous electrochemical and optical images of relatively soft samples, such as a polycarbonate membrane filter and living diatoms in a constant-current mode. This mode should be useful in mapping the biochemical activity of a living cell.**

Scanning probe microscopy (SPM) has developed dramatically in recent years because the different techniques can provide high spatial resolution (sometimes atomic) images of the structure of a surface. Some attempts to combine two or more SPM techniques have been reported in addition to studies with a single SPM technique: scanning electrochemical microscopy (SECM)/photoelectrochemical microscopy (PEM),<sup>1–3</sup> SECM/atomic force microscopy (AFM),<sup>4–10</sup> and AFM/near field scanning optical mi-

croscopy (NSOM).<sup>11,12</sup> These combinations with SECM can be applied to samples in a solution to provide chemical information in situ at different interfaces, e.g., bilayer lipid membranes and living cells. The kinetics of chemical reactions can also be studied using existing SECM theory. A technique that combines SECM and optical microscopy (OM) with simultaneous tuning-fork-based topography is described here.

We recently reported a new tip preparation and characterization procedure that allowed us to combine SECM and scanning optical microscopy (SECM/OM).<sup>13</sup> A special probe tip was constructed that consisted of a pulled optical fiber core surrounded by a gold ring and an insulating layer of electrophoretic paint. This probe could serve as not only a scanning light source but also as a microelectrode. A probe possessing structures similar to the tip used here has been reported for SECM/PEM<sup>1–3</sup> or photoelectrochemical experiments,<sup>14,15</sup> but the electrodes sizes in these studies were quite a bit larger than ours and SECM approach curves were not shown.

In SPM, the spatial resolution that is attainable is governed by both the dimension of the probe and the distance between the sample and the probe. Thus, in addition to a small probe size, another key issue in SPM is that the tip must be positioned and maintained in close proximity above the substrate. The measurement of shear force is frequently adopted to achieve this proximity between a tip and a substrate, e.g., in NSOM. For close regulation of the tip–sample separation, shear force detection using a tuning fork has often taken the place of the optical detection method<sup>16,17</sup> because it involves a more compact and simple device without the requirement of a second laser and focusing elements to measure the shear force. An analogous tuning fork application for SECM has been reported,<sup>18,19</sup> following the approach used in NSOM.<sup>16,17</sup>

- (1) Casillas, N.; James, P.; Smyrl, W. H. *J. Electrochem. Soc.* **1995**, *142*, L16–L18.
- (2) James, P.; Casillas, N.; Smyrl, W. H. *J. Electrochem. Soc.* **1996**, *143*, 3853–3865.
- (3) Shi, G.; Garfias-Mesias, L. F.; Smyrl, W. H. *J. Electrochem. Soc.* **1998**, *145*, 2011–2016.
- (4) Zhu, Y. Y.; Williams, D. E. *J. Electrochem. Soc.* **1997**, *144*, L43–L45.
- (5) Williams, D. E.; Mohiuddin, T. F.; Zhu, Y. Y. *J. Electrochem. Soc.* **1998**, *145*, 2664–2672.
- (6) Macpherson, J. V.; Unwin, P. R.; Hiller, A. C.; Bard, A. J. *J. Am. Chem. Soc.* **1996**, *118*, 6445–6452.
- (7) Jones, C. E.; Macpherson, J. V.; Unwin, P. R. *Electrochem. Commun.* **1999**, *1*, 55–60.
- (8) Macpherson, J. V.; Unwin, P. R. *Anal. Chem.* **2000**, *72*, 276–285.
- (9) Macpherson, J. V.; Unwin, P. R. *Anal. Chem.* **2001**, *73*, 550–557.

- (10) Kranz, C.; Friedbacher, G.; Mizaikoff, B.; Lugstein, A.; Smoliner, J.; Bertagnoli, E. *Anal. Chem.* **2001**, *73*, 2491–2500.
- (11) Abraham, M.; Ehrfeld, W.; Lacher, M.; Mayer, K.; Noell, W.; Guthner, P.; Barenz, J. *Ultramicroscopy* **1998**, *71*, 93–98.
- (12) Schurmann, G.; Noell, W.; Stauer, U.; de Rooij, N. F. *Ultramicroscopy* **2000**, *82*, 33–38.
- (13) Lee, Y.; Bard, A. J. *Anal. Chem.* **2002**, *74*, 3626–3633. (AC015713u).
- (14) Kuhn, L. S.; Weber, A.; Weber, S. G. *Anal. Chem.* **1990**, *62*, 1631–1636.
- (15) Pennarun, G. I.; Boxall, C.; O'Hare, D. *Analyst* **1996**, *121*, 1779–1788.
- (16) Karrai, K.; Grober, R. D. *Appl. Phys. Lett.* **1995**, *66*, 1842–1844.
- (17) Atia, W. A.; Davis, C. C. *Appl. Phys. Lett.* **1997**, *70*, 405–407.
- (18) James, P. I.; Garfias-Mesias, L. F.; Moyer, P. J.; Smyrl, W. H. *J. Electrochem. Soc.* **1998**, *145*, L64–L66.
- (19) Büchler, M.; Kelley, S. C.; Smyrl, W. H. *Electrochem. Solid-State Lett.* **2000**, *3*, 35–38.

Here, we also describe the use of a tuning fork for sensing the shear force in a combined SECM/OM. The tuning fork application allowed SECM/OM to be carried out in a constant tip–substrate distance mode. Constant-distance mode imaging has several advantages: discrimination between effects from distance variations arising from a nonflat sample or rough substrate and electrochemical surface properties<sup>20</sup> and improved lateral resolution.<sup>18</sup>

SECM imaging combined with topographic imaging has been discussed previously. SECM imaging in the contact mode with an AFM cantilever modified to make the tip conductive has been used.<sup>9</sup> In this mode, one could not measure the SECM feedback current with conductive samples because of shorting when the tip electrode touched a conductive surface. This restricted its use to insulating samples, though Kranz et al. obtained simultaneous topographical and electrochemical imaging of samples with mixed conducting and insulating features by combining the SECM functionality with an AFM tip.<sup>10</sup> To overcome these difficulties, noncontact electrochemical imaging in conjunction with contact-mode topographic imaging was developed in either a constant-height or constant-distance mode. However, in this approach, the tip had to be scanned twice over the substrate—once for SECM imaging and then for topography. Recently, the implementation of SECM in a constant-distance mode with concurrent topography based on a tuning fork was shown, although no quantitative studies on the SECM results were reported.<sup>18,19</sup> In this paper, we describe a novel SPM probe and apparatus, which can simultaneously provide electrochemical, optical, and topographic information for an interface with the use of a tuning fork.

Methods using shear force sensing have problems, especially, in imaging soft and sticky biological samples because of the strong interaction force between the probe tip and the sample. Shear force techniques can also cause breakage of the cells or deform the cell surface and move them on the substrate.<sup>21–23</sup> Thus, a reduced interaction force between the oscillating tip and the samples is required. As a solution to these problems with shear force detection, we suggest here the use of the SECM tip current as a feedback signal. We show, using SECM tip current feedback, simultaneous topographic and optical images of a membrane filter and of a biological unicellular organism, a diatom, obtained in a constant-current mode. SECM in the constant-current mode is useful for imaging soft biological cells because it keeps the advantage of a constant-distance mode but maintains a small spacing between tip and sample, thus eliminating the strong interaction force. A topographic image based on the SECM tip current feedback was obtained with an electron mediator that cannot pass through the cell wall, as previously reported.<sup>24,25</sup>

Simultaneous optical imaging was accomplished as well with the special SECM/OM probe tip described elsewhere.<sup>13</sup>

## EXPERIMENTAL SECTION

**Materials.** Ru(NH<sub>3</sub>)<sub>6</sub>Cl<sub>3</sub>·10H<sub>2</sub>O and Triton X-100 were obtained from Strem Chemicals and Aldrich, respectively. KCl (EM Industries, Inc.) was used as a supporting electrolyte. Solutions were prepared with 18 MΩ cm<sup>-1</sup> deionized water (Milli-Q, Millipore Corp. Bedford, MA) with reagent grade compounds without further purification. The test solution was 20 mM Ru(NH<sub>3</sub>)<sub>6</sub><sup>3+</sup>, 0.1 M KCl, and 0.1% Triton X-100 for all experiments. The addition of Triton X-100 helped to retard the rate of solvent evaporation, which is important in measurements with thin layers of solution. The substrate for an SECM/OM imaging experiment in the constant-force mode was an interdigitated array (IDA) electrode that had 30-μm gold bands spaced by 25-μm glass. A test substrate for the constant-current-mode imaging was a polycarbonate membrane filter (pore size, 3 μm) which was glued on the glass slide with a silicone adhesive (Anti-Seize Technology, Franklin Park, IL).

**Cell Culture.** The freshwater diatom *Navicular minima* (UTEX 391, TX) was cultured in a soil extract medium which contains 1 teaspoon of garden soil and a pinch of CaCO<sub>3</sub> in 200 mL of sterile Bristol's solution supplemented with 0.02% sodium metasilicate (Na<sub>2</sub>SiO<sub>3</sub>·9H<sub>2</sub>O). Bristol's solution was prepared with NaNO<sub>3</sub> (0.75 mg mL<sup>-1</sup>), CaCl<sub>2</sub>·2H<sub>2</sub>O (25 μg mL<sup>-1</sup>), MgSO<sub>4</sub>·7H<sub>2</sub>O (75 μg mL<sup>-1</sup>), K<sub>2</sub>HPO<sub>4</sub> (75 μg mL<sup>-1</sup>), KH<sub>2</sub>PO<sub>4</sub> (175 μg mL<sup>-1</sup>), and NaCl (25 μg mL<sup>-1</sup>). In addition to the solution media, diatoms were also cultured on an agar solid medium which was prepared by solidification of the solution containing 15 g of agar in 1 L of soil extract media. The solution mixture was microwaved after adding agar to dissolve it. This agar solution was poured into Petri dishes and solidified at room temperature. Diatoms were spread on the agar surface and cultured for one month.

**Cleaning of Diatoms.** A previously reported procedure<sup>26</sup> for cleaning diatoms was followed. Diatoms were harvested from the solution or solid media and centrifuged in 50-mL centrifuge tubes using an induction drive centrifuge (Beckmann, model J2-21M) at 3000 rpm at 4 °C for 10 min. After the upper excess medium was eliminated, the diatom precipitate was suspended in a 5% RBS-35 detergent (Pierce, Rockford, IL) solution and followed by a gentle sonication for 10 min. The partially cleaned diatoms were again pelleted by centrifugation and sonicated with new detergent solution two more times. The cleaned diatoms were rinsed and centrifuged three times in deionized water. The final pellet of diatoms was resuspended in several milliliters of water to produce the desired concentration.

**Immobilization of Cells on Glass Cover Slips.** Clean glass cover slips (VWR Scientific, Inc., Media, PA) were heated in Piranha solution at 90 °C for 10 min and rinsed and dried five times. Piranha solution was prepared as a 1:4 mixture of hydrogen peroxide (Mallinckrodt, Paris, KY) and concentrated sulfuric acid (Mallinckrodt, Phillipsburg, NJ). The cleaned glass slip was

- (20) Hengstenberg, A.; Kranz, C.; Schuhmann, W. *Chem. Eur. J.* **2000**, *6*, 1547–1554.
- (21) Lambelet, P.; Pfeffer, M.; Sayah, A. Marquis-Weible, F. *Ultramicroscopy* **1998**, *71*, 117–121.
- (22) Wadu-Mesthrige, K.; Amro, N. A.; Garno, J. C.; Cruchon-Dupeyrat, S.; Liu, G.-Y. *Appl. Surf. Sci.* **2001**, *175–176*, 391–398.
- (23) (a) Hengstenberg, A.; Blöchl, A.; Dietzel, I. D.; Schuhmann, W. *Angew. Chem., Int. Ed.* **2001**, *40*, 905–908. (b) Shevchuk, A. I.; Gorelik, J.; Harding, S. E.; Lab, M. J.; Klenerman, D.; Korchev, Y. E. *Biophys. J.* **2001**, *81*, 1759–1764. (c) Korchev, Y. E.; Raval, M.; Lab, M. J.; Gorelik, J.; Edwards, C. R. W.; Rayment, T.; Klenerman, D. *Biophys. J.* **2000**, *78*, 2675–2679. (d) Korchev, Y. E.; Gorelik, J.; Lab, M. J.; Sviderskaya, E. V.; Johnston, C. L.; Coombes, C. R.; Vodyanoy, I.; Edwards, C. R. W. *Biophys. J.* **2000**, *78*, 451–457.

- (24) Liu, B.; Rotenberg, S. A.; Mirkin, M. V. *Proc. Natl. Acad. Sci. U.S.A.* **2000**, *97*, 9855–9860.
- (25) Liu, B.; Rotenberg, S. A.; Mirkin, M. V. *J. Electroanal. Chem.* **2001**, *500*, 590–597.
- (26) Crawford, S. A.; Higgins, M. J.; Mulvaney, P.; Wetherbee, R. *J. Phycol.* **2001**, *37*, 543–554.

immersed in 0.2% polyethylenimine (PEI) (Sigma, St. Louis, MO) for 30 min, dried completely, and mounted on the bottom of a glass container. A 50- $\mu$ L sample of diatom suspension was dropped and spread onto the PEI-treated glass cover slip and allowed to adhere to the surface of the glass slip for 5 min. Then, the glass container was filled with 20 mM Ru(NH<sub>3</sub>)<sub>6</sub><sup>3+</sup>, 0.1 M KCl solution.

**Tip Preparation.** A probe tip for SECM/OM is composed of a pulled optical fiber core covered with a deposited gold layer, and an outermost insulator of electrophoretic paint, forming a ring-shaped electrode. The detailed method for tip fabrication is described elsewhere.<sup>13</sup> This tip was mounted on one prong of a quartz crystal tuning fork (32.768 kHz, X801-ND, Digi-Key, Thief River Falls, MN) and glued with Torr-seal (Varian) while the tip protruded  $\sim$ 1 mm beyond the end of tuning fork; only this extended part of the tip was immersed into solution while the tuning fork remained in air during experiments. The tip attached to the tuning fork was dried at  $\sim$ 50 °C in the oven for  $\sim$ 4 h. We found, in agreement with a recent report on NSOM imaging in liquids, that immersion of the tuning fork itself led to severe degradation of the response.<sup>27</sup> Details of these experiments are given in the Supporting Information.

**Instrumentation.** The instrumental setup for SECM/OM shown in Supporting Information is very similar to the previous one<sup>28</sup> for scanning optical microscopy using electrogenerated chemiluminescent (ECL) light at a nanotip with the addition of optical devices. The program to control this home-built SECM/OM system and to acquire data was designed using LabVIEW (National Instruments, Austin, TX).

For SECM, we used a two-electrode system; the working electrode was the ring electrode and the reference electrode was Ag/AgCl. As a light source, an Innova 90 argon ion laser (Coherent) at wavelength 514 nm was coupled to the other end of the optical fiber probe tip. The tip was mounted perpendicular to the substrate with a holder. All experiments were accomplished in a darkbox to protect the system from the interference of ambient light. The transmitted light through the substrate was detected with a photomultiplier tube (PMT) (model R4220P, Hamamatsu), which was placed under the substrate, and the generated current was measured with a Keithley model 6517 electrometer.

The movement of the tip was controlled by three inchworm motors (Burleigh Instruments) as well as a 40- $\mu$ m piezoelectric pusher (Burleigh) for fine resolution in the  $z$  direction. This pusher provides a 4- or 8-nm retraction (depending on gain setting) for a 5-mV increase in applied voltage. Therefore, the applied pusher voltage can be correlated with the topography of the sample.

**Constant-Force Mode.** Shear force detection using a tuning fork was employed for feedback for tip–substrate distance ( $d$ ) regulation. A piezoelectric tube drives the oscillation of the attached tuning fork at its resonance frequency, and the generated piezoelectric potential correlating with this vibration amplitude is monitored with a lock-in amplifier (EG&G Princeton Applied Research, model 5210). After coarse tip approach with an inchworm, the tip was moved toward the substrate using a pusher in a fine-resolution mode (4-nm approach/ms) until the monitored

tuning fork amplitude damped to the set point (taken as 95–97% of the original amplitude). At this point, the tip is very close to or touching the substrate. The tip was stopped, retracted by 24 nm (in 1 ms), and then the tip current, transmitted light intensity, and applied pusher voltage were measured simultaneously. In this way, a constant-interaction force between the probe and the substrate, or a constant tip-to-substrate distance, was maintained. This procedure was repeated after the tip moved 80 nm in the  $x$  direction (40 ms) until the tip traveled over the whole scan length. It took 47 ms for a single 80-nm scan in the  $x$ -axis direction in this mode. Basically, in terms of a scanning method, this tapping-mode-like system allowed SECM/OM to be used in a constant-distance mode. This scanning method, as a function of time, is shown in the Supporting Information. With this mode, 8-nm retractions correspond to 5-mV increases in applied voltage to the pusher.

**Constant-Current Mode.** For imaging in the constant-current mode, the SECM tip current rather than the tuning fork amplitude was used to control the tip–sample separation. This constant current corresponds to a fixed tip–substrate distance that can be calculated from SECM theory, when the tip is above an insulator. The SECM tip current (instead of tunneling current in electrochemical STM<sup>29</sup>) was monitored as a function of the displacement of the tip in the  $z$ -axis direction as the tip approached the insulating sample. This approach was stopped when the tip current decreased to a preset value, which was usually a 20–30% decrease from the steady-state tip current ( $i_{T,\infty}$ ). The tip was then scanned over the sample in the  $x$  and  $y$  directions while the tip position in the  $z$  axis was changed to maintain the tip current within  $\sim$ 1% of the set point. The applied pusher voltage for topographic imaging and the transmitted light intensity for optical imaging were measured simultaneously. With this pusher, 8-nm retractions correspond to 5-mV increases in the applied voltage. Therefore, the applied pusher voltages are a measure of the topography of the sample. The PMT was located right under the glass container to measure the transmitted light intensity from the tip positioned above a glass slide.

## RESULTS AND DISCUSSION

**SECM/OM in Constant-Force Mode. SECM/OM Approach Curves on a Glass Slide.** As the tip was moved toward a flat glass substrate, the amplitude of the tuning fork vibration at its resonance frequency ( $\sim$ 32 kHz), the tip current, and the light intensity beneath the substrate were measured simultaneously as a function of the tip–glass substrate distance. This allowed the measurement of force, SECM, and optical approach curves, simultaneously. These approach curves are shown in Figure 1.

The measured amplitude of the tuning fork vibration at its resonance frequency was used as feedback for controlling the tip–substrate distance ( $d$ ). This amplitude showed a very sharp damping when the tip touched the substrate within 4 nm in the  $z$  direction (Figure 1a). The increment 4 nm was the minimum value in the  $z$ -axis movement limited by the  $Z$ -pusher resolution and the LabVIEW program. The 3–5% decrease of amplitude of tuning fork oscillation compared to the original amplitude (when the tip

(27) Lee, L. F.; Schaller, R. D.; Haber, L. H.; Saykally, R. J., *Anal. Chem.* **2001**, *73*, 5015–5019.

(28) Zu, Y.; Ding, Z.; Zhou, J.; Lee, Y.; Bard, A. J. *Anal. Chem.* **2001**, *73*, 2153–2156.

(29) Bard, A. J.; Faulkner, L. R. *Electrochemical Methods*, 2nd ed.; Wiley: New York, 2001.

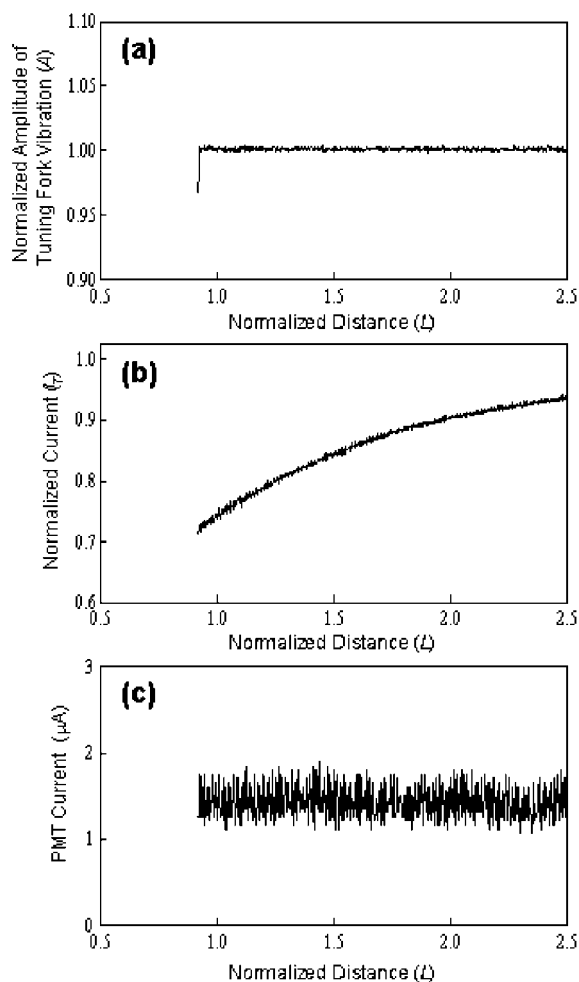


Figure 1. Simultaneously obtained (a) force, (b) electrochemical, and (c) optical approach curves for a glass substrate. *a*, *b*, and  $r_g$  of the tip were 0.62, 0.7, and 1.75  $\mu\text{m}$ , respectively.

is positioned far from the substrate) was set to prevent the tip from pushing further toward the substrate.

In the SECM approach curve (Figure 1b), the tip current did not fall to zero at the point where the tuning fork oscillation became damped. At that point, the tip still looked as if it was far from the substrate in terms of the SECM response, although the force approach indicated that the tip really touched the glass substrate. This observation can be attributed to either the nature of the tip geometry at the bottom of the tip or of the tip not being moved perpendicular to the substrate surface, or both. If the shape of a tip is conelike rather than a flat ring, even when the bottom of the tip touches the substrate,  $\text{Ru}(\text{NH}_3)_6^{3+}$  in solution can still access the electrode area in the way shown in Figure 2a. This behavior can be observed similarly in the case of a ring-shaped tip if the insulating sheath is thick and the angle between the plane of the tip and the substrate deviates from  $90^\circ$  so that the insulator touches the substrate before the metal electrode area touches (Figure 2b). In either case, the electrode is not completely blocked from access of  $\text{Ru}(\text{NH}_3)_6^{3+}$  to the metal portion of the tip when the substrate is touched. As shown in the next section, the former case (Figure 2a) seems the most important, because the approach curves show a good fit to the simulated ones of ring electrode.

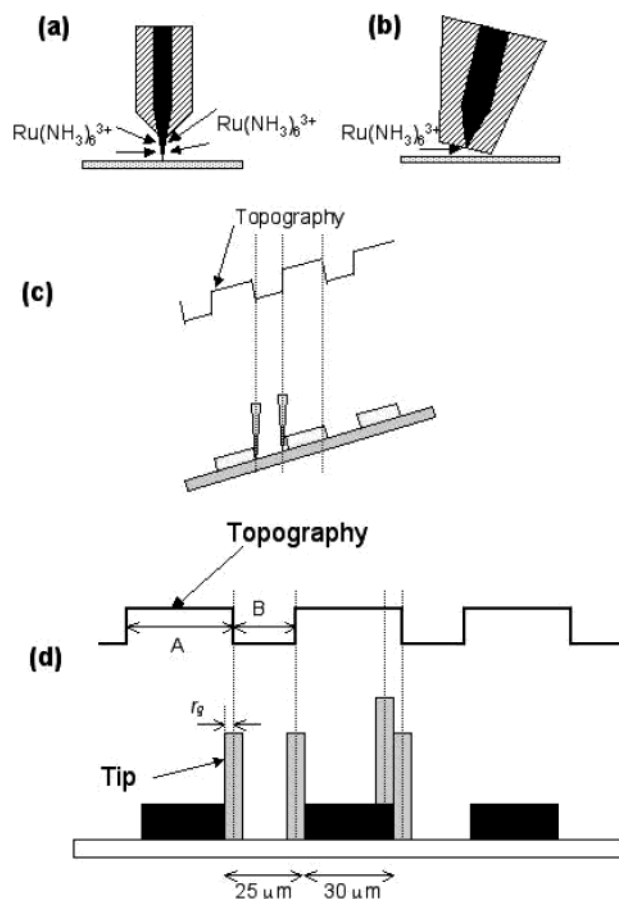


Figure 2. Schematic representation showing possible reasons for the difference in the zero point obtained from shear force and SECM because of access of  $\text{Ru}(\text{NH}_3)_6^{3+}$  in solution to the electrode area of a tip when the tip contacts the substrate surface: (a) protruding tip; (b) tilted substrate. Schematic representation of the effect of a tilted substrate surface on topographic imaging (c). Schematic of how topographic image is limited by the outermost diameter of the tip (d).

The intensity of light coming from the optical fiber core of the tip was measured with a PMT located under the glass substrate as a function of tip–substrate distance (Figure 1c). There was no intensity change of light transmitted as the tip approached, showing that all of the light from the tip was collected by the PMT independent of how far the tip was positioned from the substrate.

**SECM Approach Curves on Gold and Glass Substrates of an IDA.** The experimental SECM approach curves at conductive or insulating substrates agreed very well with the theoretical ones for a ring electrode (Figure 3). We recently showed how SECM approach curves for a ring electrode depend on the thickness of the ring and insulating sheath and reported a method of determining the geometry and size of a ring electrode.<sup>30</sup> This configuration was very similar to the tip in this experiment, so by comparing experimental and theoretical SECM curves, the dimensions of the tip could be established using this technique. The results are as follows: 620, 700, and 1750 nm for the inner (a) and outer (b) radii of the ring and the outermost radius ( $r_g$ ) of insulating sheath, respectively.

As mentioned above, at the point the tuning fork response damped suddenly, the SECM curves showed that the tip was still

(30) Lee, Y.; Amemiya, S.; Bard, A. J. *Anal. Chem.* **2001**, *73*, 2261–2267.

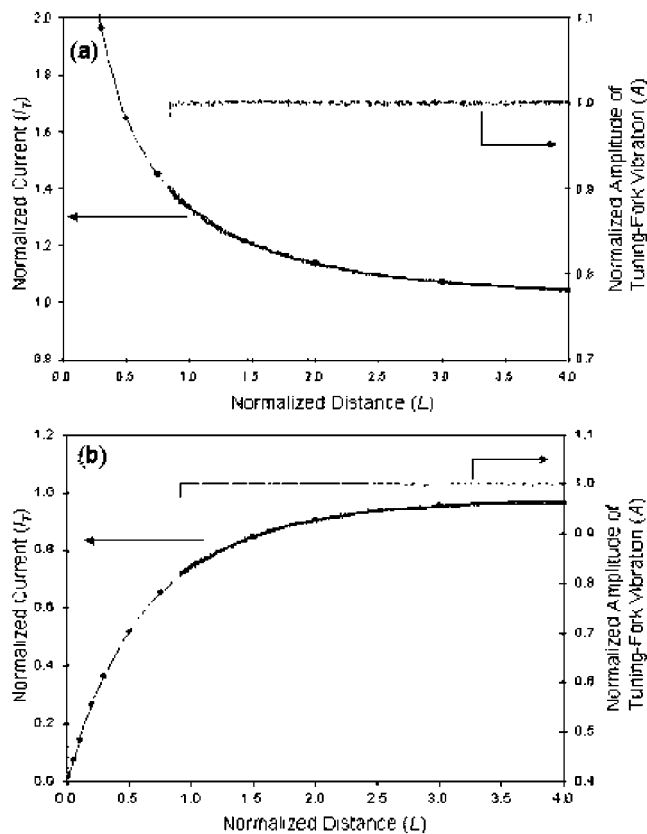


Figure 3. Comparison of experimental and theoretical SECM curves at (a) gold and (b) glass substrates. Theoretical curves (dotted lines) for  $a/b = 0.9$  and  $r_g/b = 2.5$ . Normalized experimental curves (solid lines) in an aqueous solution containing 20 mM  $\text{Ru}(\text{NH}_3)_6^{3+}$ , 0.1 M KCl, and 0.1% Triton. Normalized distance ( $L = d/b$ ). Upper curves are the simultaneously obtained force approach curves.  $a$ ,  $b$ , and  $r_g$  of the tip were 0.62, 0.7, and 1.75  $\mu\text{m}$ , respectively.

a finite distance from the substrate, either an insulator or a conductor. We regard the sharp amplitude decrease of tuning fork oscillation as the point at which some part of the tip contacts the substrate. Figure 3 shows that these contact points were matched within  $\Delta L \approx 0.04$  for both substrates:  $I$  (the normalized current  $= I_T/I_{T,\infty} \approx 0.88$  and  $0.92$  for the gold and glass substrates, respectively). Considering the small radius of the tip, a 0.04 difference in  $L$  represents only  $\sim 28$  nm, which can arise from a tilted substrate or surface roughness relative to the tip. Since the experimental SECM approach curves for both conductive and insulating substrates matched fairly well the theoretical ones for a ring-shaped electrode, the tip geometry is close to a ring. The fact that the SECM tip current was not zero at the physical contact point can thus be attributed to a tilted substrate (Figure 2b) rather than a cone-shaped tip geometry (Figure 2a). At the contact point, the tip current showed a 39% increase (for the gold substrate) and a 27% decrease (for the glass substrate) compared to the steady-state current ( $I_{T,\infty}$ ) at  $d \rightarrow \infty$ . In other words, the probe size (with an outermost radius of 1.75  $\mu\text{m}$ ) is not small enough for the gold ring electrode to approach very close to the substrate without the insulator touching.

**Single Line Scan of an IDA Electrode.** Before imaging samples, simultaneous single lateral line scanning was performed for an IDA electrode consisting of 30- $\mu\text{m}$  deposited gold fingers spaced by 25- $\mu\text{m}$  glass areas in an aqueous solution containing

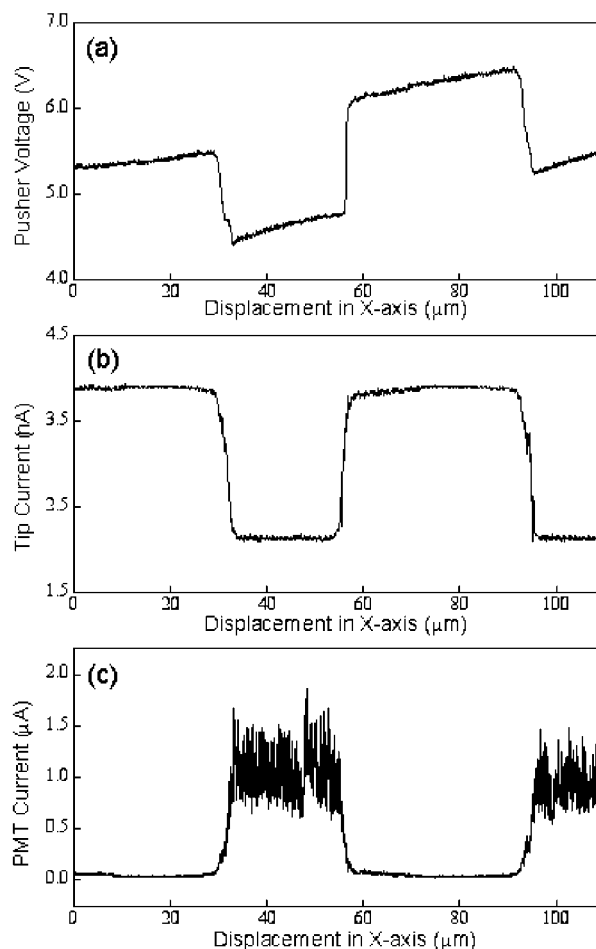


Figure 4. Simultaneous (a) topographic, (b) electrochemical, and (c) optical single line scans in constant-distance mode using a double-insulated tip over an IDA electrode in an aqueous solution containing 20 mM  $\text{Ru}(\text{NH}_3)_6^{3+}$ , 0.1 M KCl, and 0.1% Triton; 30- $\mu\text{m}$  gold bands spaced by 25- $\mu\text{m}$  glass.  $a$ ,  $b$ , and  $r_g$  of the tip were 0.62, 0.7, and 1.75  $\mu\text{m}$ , respectively. With this mode, 8-nm retractions of the pusher correspond to 5-mV increases in applied voltage.

20 mM  $\text{Ru}(\text{NH}_3)_6^{3+}$ , 0.1 M KCl, and 0.1% Triton using the procedure shown Figure 2 in the Supporting Information. Figure 4 shows simultaneous single line scans obtained with a good double-insulated tip. For topography, the applied pusher voltages were measured to maintain the set point. The thickness of the deposited gold layer of the IDA electrode was  $\sim 0.92$   $\mu\text{m}$  from the topographic single line scan, (5-mV pusher voltage changes per 4-nm height changes). A simultaneous SECM line scan exhibited positive feedback over the gold layers and negative feedback over the glass and corresponded to the topographic scan. The optical line scan was also consistent with both the SECM and topographic line scans; transmitted light was observed only for the glass zones but not for the gold layers.

The topographic single line scan over the IDA electrode substrate showed this substrate was tilted with the right side higher than the left. This tilt also supports the tilted substrate explanation (shown in Figure 2b) rather than the conical electrode one (Figure 2a). Another expected effect of the tilted substrate is the asymmetric topography for the gold band/glass edges as illustrated in Figure 2c. This predicted behavior was observed: a gentler downward slope (gold to glass) than upward slope (glass

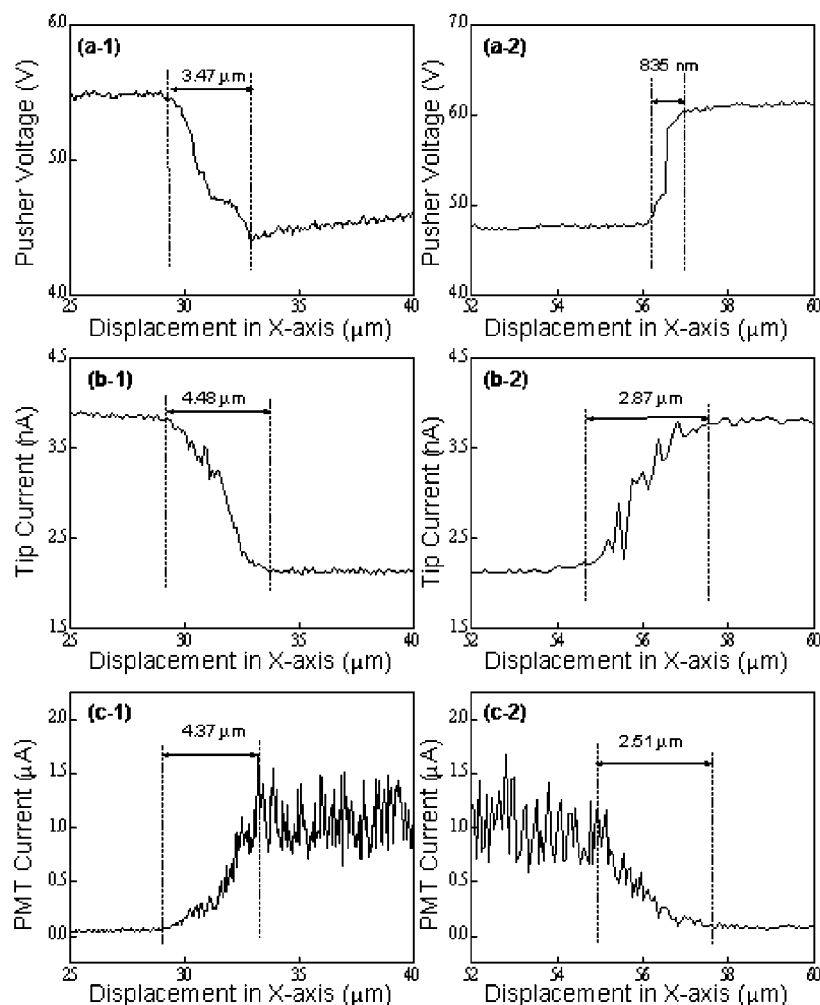


Figure 5. Comparison of upward and downward gold/glass edges for a tilted substrate in simultaneous (a) topographic, (b) electrochemical, and (c) optical single line scans in a constant-distance mode over an IDA electrode: 30- $\mu\text{m}$  gold bands spaced by 25- $\mu\text{m}$  glass.  $a$ ,  $b$ , and  $r_g$  of the tip were 0.62, 0.7, and 1.75  $\mu\text{m}$ , respectively; 5-mV pusher voltage corresponds to 8 nm of distance change.

to gold) in the topographic line scan (Figure 5a). The uphill was  $\sim 840$  nm wide while the width of the downhill was  $\sim 3.5$   $\mu\text{m}$ . This was also true for both SECM and optical scans (Figure 5b and c, respectively). The resolution for the gold/glass edges was lower with the SECM and optical line scans than in the topographic line scan mode. The resolution in the optical line scanning could not attain that of NSOM, even when the tip was positioned within the near-field region ( $\sim 24$  nm) over the substrate. This can be ascribed to the aperture size of the optical core in the center of the tip. The estimated core diameter using SECM approach curves (see the previous section) was 1.3  $\mu\text{m}$ , which is much larger than the wavelength (514 nm) of the laser light and that needed for a good NSOM tip.

Since the line scans were obtained by a tapping-mode-like scanning of the tip, this mode can be considered as SECM/OM in a constant-distance mode. Except for the asymmetry between gold to glass and glass to gold at the edges, as mentioned above, the measured SECM line scan was not influenced by the tilted IDA substrate, as expected for a constant-distance mode.<sup>9,20</sup> In other words, the positive or negative feedback currents were quite uniform throughout the line scan, even when a simultaneous topographic line scan revealed an inclined substrate plane. The measured tip currents were 3.8 and 2.1 nA over gold and glass,

respectively; i.e., the tip current showed a 36% increase and a 25% decrease relative to 2.8 nA ( $i_{T,\infty}$ ) for the gold and glass substrates, respectively. These larger or smaller values were slightly less in magnitude than when a tip "contacted" the substrate; a 39% increase for platinum and a 27% decrease for glass (Figure 3). This can be attributed to the fact that the tip was retracted after touching the substrate surface before acquiring SECM feedback current.

**Imaging an IDA Electrode.** Figure 6 shows simultaneous topographic, electrochemical, and optical images of an IDA electrode. These images were obtained as follows. After finishing a single line scan of the  $x$  axis, the tip was moved 2.5  $\mu\text{m}$  on the  $y$  axis in the same way as used for single line scanning, i.e., a tapping-mode-like constant-distance mode. Then, the tip traveled back along the  $x$  axis for another single line scan over the substrate, followed by another 2.5- $\mu\text{m}$  increment in the  $y$  axis. These steps were repeated for imaging the substrate at interest.

When the tip was located above a gold band (higher in topography), the SECM feedback current increased and the optical signal, the intensity of transmitted light, detected under the substrate, dropped to almost zero. When the tip was positioned over a glass area, the opposite responses were observed. Thus, the bright part in topographic and SECM images appeared dark

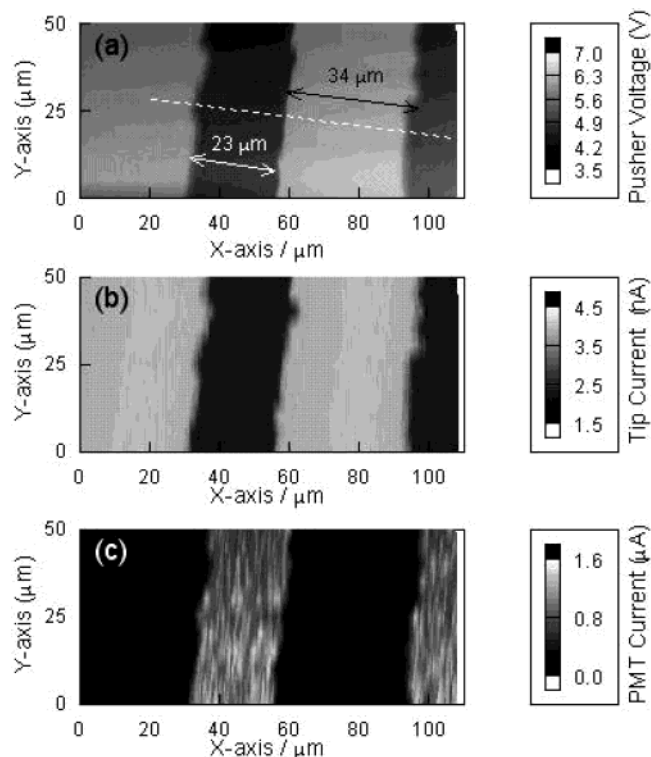


Figure 6. Simultaneously obtained (a) topographic, (b) electrochemical, and (c) optical images with the constant-distance mode over an IDA electrode: 30- $\mu\text{m}$  gold bands spaced by 25- $\mu\text{m}$  glass. *a*, *b*, and *c* of the tip were 0.62, 0.7, and 1.75  $\mu\text{m}$ , respectively. Scan speed was 1  $\mu\text{m s}^{-1}$ ; 5-mV pusher voltage corresponds to 8 nm of distance change.

in the optical images as shown in Figure 6. These images showed an apparently higher spatial resolution compared to the images obtained in the fixed-height mode.<sup>13</sup>

In addition to a close spacing between the tip and substrate, lateral resolution in topography is governed by the size of the probe tip including the insulating sheath.<sup>20</sup> This can be seen in Figure 6a. The width of gold bands (*A*) and glass (*B*) were  $\sim 34$  and  $\sim 23$   $\mu\text{m}$ , respectively. The structure estimated by topography has a wider gold band and a narrower glass band compared to the actual IDA structure, 30- $\mu\text{m}$  gold and 25- $\mu\text{m}$  glass, while the sum of a gold band and glass (57  $\mu\text{m}$  wide) was slightly larger than 55  $\mu\text{m}$ . The tip size can be extracted from the obtained topography, because  $A = 30 \mu\text{m} + 2r_g$ , and  $B = 25 \mu\text{m} - 2r_g$  in Figure 2d. The outermost insulator sheath radius ( $r_g$ ) was calculated as 1–2  $\mu\text{m}$ , which matched very well with  $\sim 1.75$   $\mu\text{m}$  obtained using SECM approach curves as described in the previous section.

One shortcoming of this system comes from this tapping-mode-like scanning mode. The tip can be easily damaged during experiments because of the frequent contact with the substrate. For example, the tip will touch the substrate surface 1250 times for each 100- $\mu\text{m}$  single line scan. This leads to significant deterioration of the tip, and this is even worse during *x*–*y* imaging.

**Imaging Diatoms.** The diatoms (class Bacillariophyceae) are a group of single-cell photosynthetic algae abundant in various seawater and freshwater environments.<sup>31</sup> They are encased in a porous silica structure called the frustule. Generally there are two major groups of diatoms: sphere-shaped diatoms that exhibit

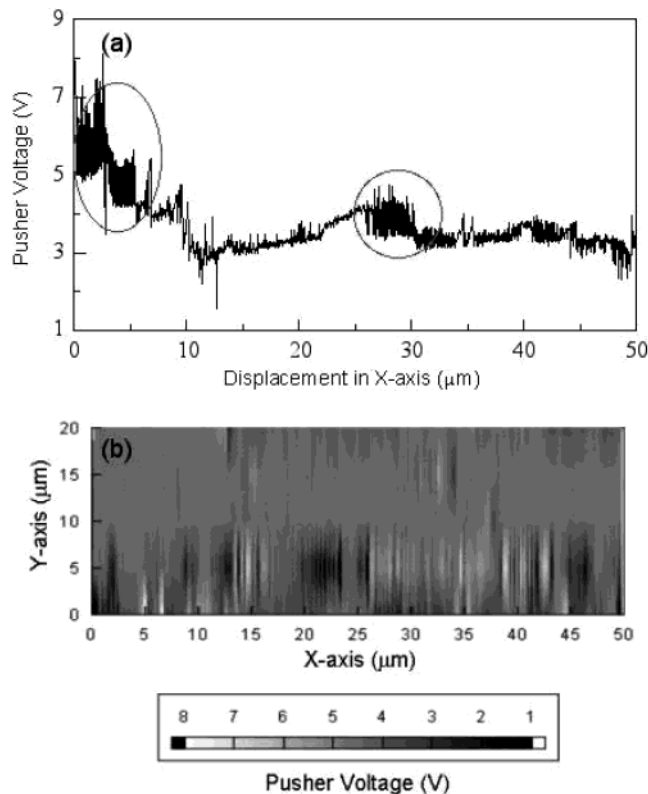


Figure 7. (a) Topographic lateral single line scan based on a tuning fork for diatoms immobilized on a glass substrate under water at a scan rate of 1  $\mu\text{m s}^{-1}$ . (b) Topographic image based on a tuning fork for diatoms immobilized on a glass substrate under water at a scan rate of 1  $\mu\text{m s}^{-1}$ . *a*, *b*, and *c* of the tip were 0.75, 0.83, and 1.7  $\mu\text{m}$ , respectively.

radial symmetry and cylinder-shaped diatoms that are bilaterally symmetrical.<sup>31</sup> Figure 10 shows optical microscope images of *N. minima* diatoms immobilized on PEI-treated glass. This diatom has a cylindrical shape. Generally the cell size of diatoms decreases through the life cycle of these organisms. Thus, as shown in Figure 3 in the Supporting Information, *N. minima* exhibits a distribution of sizes within the range 3–4  $\mu\text{m}$  wide and 4–12  $\mu\text{m}$  long.

A topographic lateral single line scan above the diatom cells immobilized on glass under solution was obtained at a scan rate of 1  $\mu\text{m s}^{-1}$ . (Figure 7a) The parts that show higher pusher voltages (circled regions in Figure 7a) suggest the presence of cells. In those parts, the measured pusher voltage signals appeared with significant noise; i.e., the position of the tip in the *z* axis controlled by sensing the amplitude damping of the tuning fork vibration was particularly unstable over the cells. This fluctuating tip position in the *z* axis was not observed with harder samples such as the interdigitated array (IDA) electrode. On the other hand, similar behavior has been observed for biological samples possessing soft cell surfaces because of the strong interaction force between a vibrating tip and sample.<sup>23</sup> Imaging of soft biological cells with shear force detection has been reported; however, a separate aligned photodiode and a laser were needed to detect the damping of the vibration of electrodes.<sup>23a</sup> Although

(31) For a review of diatoms, see: Pickett-heaps, J.; Schmid, A.; Edgar, L. A. In *Progress in Phycological Research*; Round, F. E., Chapman, D. J., Eds.; Bristol: 1990.

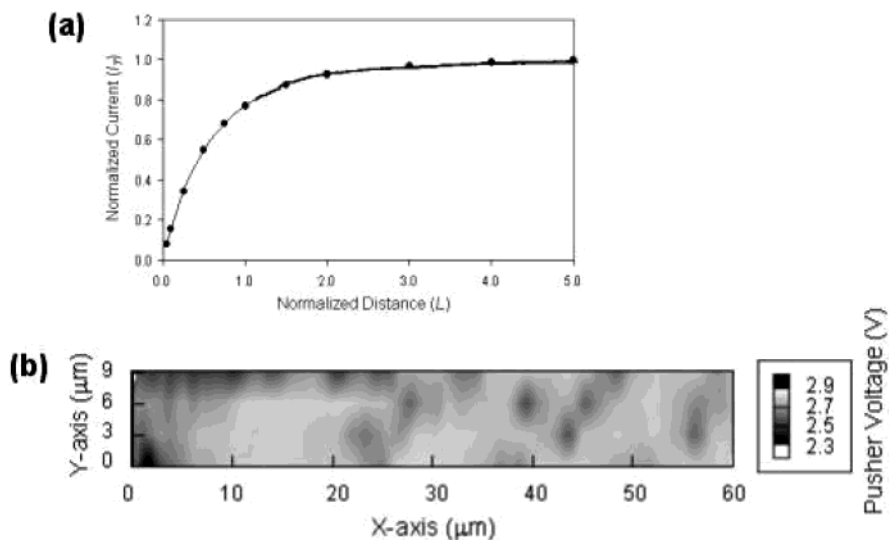


Figure 8. (a) Comparison of the experimental and theoretical SECM approach curves for a membrane filter. Theoretical curves (dotted lines) for  $a/b = 0.85$  and  $r_g/b = 2$ . Normalized experimental curves (solid lines) in aqueous solution containing 20 mM  $\text{Ru}(\text{NH}_3)_6^{3+}$  and 0.1 M KCl using a SECM/OM tip. The estimated tip size is 0.5, 0.7, and 1.5  $\mu\text{m}$  for the inner (a) and outer (b) radii of a ring and the outermost radius of insulating sheath ( $r_g$ ), respectively. Normalized distance ( $L$ ) =  $d/b$  and normalized current ( $i_T$ ) =  $i_T/i_{T,\infty}$ . Tip approach to the substrate stopped when the tip current decreased to 80% of  $i_{T,\infty}$ . (b) SECM images representing topography of a membrane. The scan area is 60  $\mu\text{m} \times 9 \mu\text{m}$ , imaged at a scan rate of 1  $\mu\text{m s}^{-1}$ .  $a$ ,  $b$ , and  $r_g$  of the tip were 0.5, 0.7, and 1.5  $\mu\text{m}$ , respectively; 5-mV pusher voltage corresponds to 4 nm of distance change.

the silicate diatom frustule should be quite hard, the exterior of the frustule is covered with an organic glue-like material that forms soft and sticky thin layers over the silicate wall.<sup>26</sup> Thus, the nature of the interaction between the tip and these organic layers will probably be similar to those for soft biological cells. Moreover, the tapping-mode-like movement of the tip for imaging can easily affect the outermost surface morphology of the cells. This mucilage layer on the diatoms has been reported to peel off and pile up during tip sweeps over the diatoms in contact-mode AFM.<sup>26</sup> Because of this strong interaction, topographic imaging based on tuning fork dithering was not good enough to distinguish the cells in the image obtained as shown in Figure 7b. This fuzzy topographic image may represent a damaged outermost layer of the cells caused by movement of the tip on top of the cell surface.

**SECM/OM in the Constant-Current Mode.** To achieve imaging in a constant-current mode, the tip was held at a sufficiently negative potential to reduce an electroactive species in solution,  $\text{Ru}(\text{NH}_3)_6^{3+}$ , that cannot pass through the diatom cell wall. Thus, a negative feedback current is expected above the diatoms as well as above the glass substrate. The tip current was then monitored as a function of the displacement of the tip in the  $z$  direction when the tip approached the sample. This approach was stopped when the tip current attained a 20–30% decrease (set point) from the steady-state tip current ( $i_{T,\infty}$ ). The tip was then scanned over the sample in the  $x$  and  $y$  directions while the tip current was maintained within  $\sim 1\%$  of the set point. During scanning, the pusher voltage, representing the height variation of the sample, was measured for topographic imaging. At the same time, the PMT current was also measured for optical imaging. The most important feature in the constant-current mode is the stability of  $i_{T,\infty}$  as a function of time because the tip current was used as the feedback signal to regulate the tip–sample separation. The tip used here showed excellent stability of  $i_{T,\infty}$ , which was constant over several hours in solution.

**Membrane Filters.** For a test imaging experiment in the constant-current mode, polycarbonate membrane filters (Osmonics, Livermore, CA), with a pore size of 3  $\mu\text{m}$ , glued on a glass slide with a silicone adhesive (Anti-Seize Technology, Franklin Park, IL) were used as an insulating sample with a known structure. The membrane was immersed in 20 mM  $\text{Ru}(\text{NH}_3)_6^{3+}$  and the diffusion-controlled steady-state current for the reduction of  $\text{Ru}(\text{NH}_3)_6^{3+}$  was monitored. When the tip was far from the sample surface,  $i_{T,\infty}$  was  $\sim 3$  nA corresponding to the tip size. The tip dimension was determined by the SECM method described elsewhere<sup>30</sup> as 0.5, 0.7, and 1.5  $\mu\text{m}$  for the inner (a) and outer (b) radii of a gold ring and the outermost radius of insulating sheath ( $r_g$ ), respectively.

Information about the tip–sample distance can be extracted by comparison of the normalized experimental and theoretical SECM approach curves (Figure 8a), with knowledge of the tip size. When the tip current decreased to 80% (set point) of  $i_{T,\infty}$ , the normalized distance in the  $z$  direction ( $L = d/b$ ) was  $\sim 1$ , equivalent to a 0.7- $\mu\text{m}$  ( $d$ ) separation from the sample (outer ring radius, 0.7  $\mu\text{m}$ ). This tip current was sustained with a 1% variation of the set tip current while the tip was scanned over the membrane in the  $x$  and  $y$  directions to obtain an SECM image in the constant-current mode. The SECM images obtained representing topography of a membrane are shown in Figure 8b. The scan area was 60  $\mu\text{m} \times 9 \mu\text{m}$ , imaged at a scan rate of 1  $\mu\text{m s}^{-1}$ . The SECM feedback current became larger when the tip was positioned over a hole rather than a polycarbonate sheet, because of lower blocking of the membrane for the diffusion of electroactive species to the tip. Therefore, the feedback control moves the tip closer to the membrane to maintain the constant current. The polycarbonate sheet (thickness, 10  $\mu\text{m}$ ) is definitely thicker than the tip–sample separation ( $\sim 700$  nm), so the tip must have traveled into the holes. The tip diameter including insulator sheath was  $\sim 2.8 \mu\text{m}$ , similar to the pore size. As explained in the previous



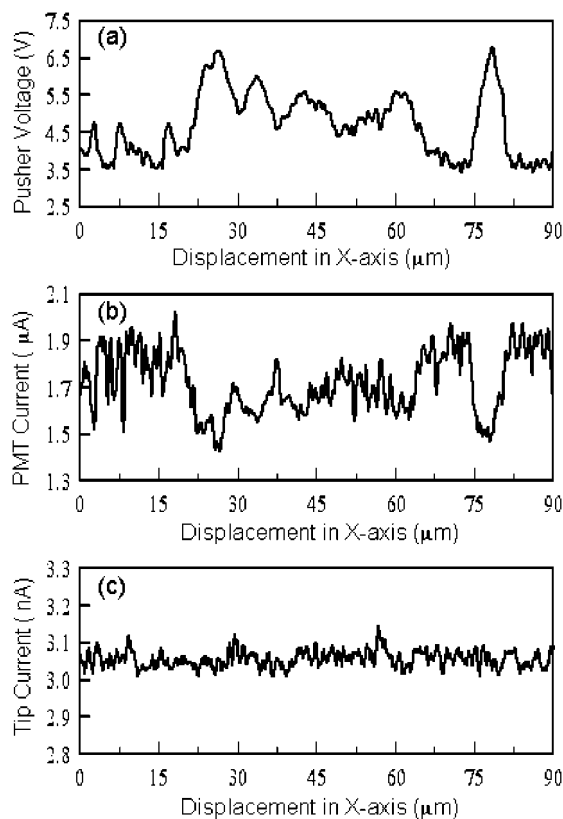


Figure 9. Simultaneously obtained (a) SECM and (b) optical single line scans over diatoms at a scan rate of  $1 \mu\text{m s}^{-1}$ . (c) shows the constancy of the current throughout the total line scan.  $a$ ,  $b$ , and  $r_g$  of the tip were 0.65, 0.72, and  $1.5 \mu\text{m}$ , respectively. Correlation between pusher voltage and distance traveled is the same as in Figure 8.

section, because of the dependence of topography on the shape and particularly the physical size of a tip, the holes appear a little smaller than their actual size. However, the holes were recognizable and that confirmed the possibility of SECM imaging in a constant-current mode.

**Diatoms.** SECM and optical images of the freshwater diatoms (*N. minima*) were obtained by the same approach as with the membrane filters. Figure 9 shows simultaneously obtained single line scans for topography (a), optical transmittance (b), and SECM tip current (c) at a scan rate of  $1 \mu\text{m s}^{-1}$ . Figure 9c verifies that the tip current is maintained at a constant value through the whole tip scan. On the other hand, the voltages applied to the pusher (Figure 9a), which represents the tip position on the  $z$  axis, changed when the tip moved in the  $x$  direction. Because all parts of the sample, i.e., the silicate cell walls of the diatom frustule, as well as the glass substrate are insulators, negative feedback is expected over all areas of the substrate. Therefore, the recorded tip height based on a constant SECM current corresponds directly to the topography of the substrate. The optical lateral scan (Figure 9b) obtained simultaneously appeared the exact opposite of the topographic scan; the higher the voltage in the topographic lateral scan, the lower the light intensity in the optical one. The reduced light intensity where the topographic scan shows a high altitude represents the presence of a cell, because the transmitted light, which is measured using the PMT under the sample for the optical lateral scan, is blocked by the cells.

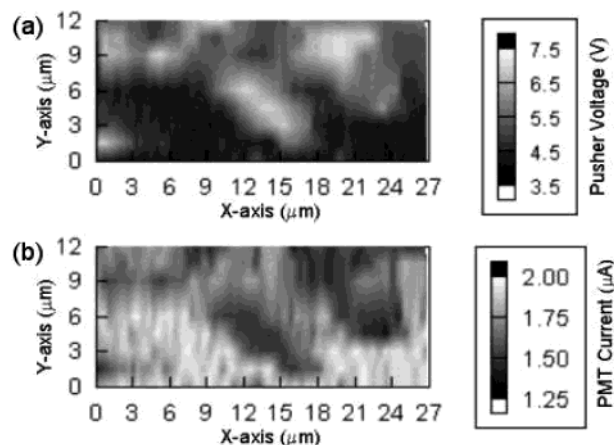


Figure 10. Simultaneously obtained (a) SECM and (b) optical images over diatoms at a scan rate of  $1 \mu\text{m s}^{-1}$ .  $a$ ,  $b$ , and  $r_g$  of the tip were 0.65, 0.72, and  $1.5 \mu\text{m}$ , respectively. Correlation between pusher voltage and distance traveled is the same as in Figure 8.

Panels a and b of Figure 10 show, respectively, the topographic and optical images of the diatoms obtained simultaneously using a SECM/OM tip. The characterized tip size was similar to the one used for imaging the membrane filter in the previous section. The scan area was  $27 \mu\text{m} \times 12 \mu\text{m}$ , imaged at a scan rate of  $1 \mu\text{m s}^{-1}$ . As noticed in the lateral single line scan, the optical image corresponds to the topographic image with the opposite pattern. The existence of a unicellular diatom in the middle of the imaged area is clear. The highest height of that diatom was measured as  $\sim 5.0 \mu\text{m}$  from the applied pusher voltage. The measured width of the same diatom cell from the image was  $\sim 4.5 \mu\text{m}$  while the length was  $\sim 9 \mu\text{m}$ . The cylindrical shape and size ( $\sim 5\text{-}\mu\text{m}$  diameter and  $\sim 9\text{-}\mu\text{m}$  length) of the diatom, determined by SECM/OM, agrees quite well with that observed in a light optical microscope image.

Compared to the topographic image obtained in the constant-force mode using a tuning fork, the image in the constant SECM current mode was certainly better; it shows a clear image of the diatoms while these cells could not be recognized in the image based on a tuning fork height control. This better performance with the constant-current mode can be explained as follows. In the constant-current mode, the tip is not oscillating so that the perturbing strong interaction between the tip and soft samples no longer exists. In addition, the tip-sample separation is larger in the constant-current mode than with shear force detection; i.e., SECM is a noncontact mode of imaging. Deformation of the cells by touching with the tip is thus avoided in the constant-current mode. On the other hand, too large a tip-sample separation prevents high-resolution imaging. Therefore, the optimum distance between the tip and sample, which allows imaging without damaging the samples, but with high resolution, needs to be achieved for imaging biological samples.

In our system, imaging in the constant-current mode is restricted to the samples, which consist of only insulating (or only conducting) samples. In other words, the SECM current has to show only negative feedback (or only positive feedback) through a whole scan area since only a change of a tip current in one direction (either decrease or increase) is monitored as a feedback signal to regulate a tip-sample distance. However, the constant-current mode is generally useful for biological samples since they

are all insulators (in the electroactive molecule SECM sense). The resolution obtained so far is not sufficiently high to image the pores in the diatom frustule so that smaller tips, smaller spacings, and faster feedback control is needed to perform high-resolution imaging.

## CONCLUSIONS

Combined scanning electrochemical and optical microscopy has been demonstrated with two different methods of regulating the tip-sample distance: constant-force and constant-current modes. As a probe tip, a ring microelectrode consisting of an optical fiber core, a gold ring, and an insulator was used. It served well as an ultramicroelectrode for SECM and as a light source for OM when coupled to a laser. In the constant-force mode, a quartz crystal tuning fork (32.768 kHz) was used for detecting the shear force, which was employed as a feedback signal to control the tip-substrate separation. The shear force detection method provided simultaneous tuning fork-based topographic imaging in addition to the electrochemical and optical images of the samples in a tapping-mode-like constant-distance mode. The consistent acquisition of simultaneous topographic, electrochemical, and optical images of an IDA electrode demonstrated the capability of SECM/OM. SECM feedback imaging of quite an uneven substrate (the thickness of the gold fingers of the IDA on the glass surface was  $\sim 0.92 \mu\text{m}$ ) that consisted of conductive as well as insulating zones was successfully performed without problems of shorting or the effect of substrate tilt. An improved lateral resolution for both optical imaging and SECM imaging was achieved in a constant-distance mode rather than with a fixed-height mode. This can be attributed to a closer proximity of the tip to the substrate in the constant-distance mode. This technique can be applied to obtain simultaneous electrochemical, optical, and structural information about interfaces. With the construction of a smaller tip, an improved spatial resolution should be possible, leading to NSOM combined with SECM and simultaneous topography.

In constant-current-mode imaging, the SECM feedback current was used as the feedback signal to regulate the tip-sample

separation instead of the shear force. We report the first successful simultaneous topographic and optical imaging of a living unicellular organism by the constant SECM current mode as a feasible solution for imaging soft biological samples. Topography of the freshwater diatoms, *N. minima*, could not be imaged clearly with the shear force detection using a tuning fork because of the strong interaction force between the vibrating tip and diatoms. On the other hand, the diatoms were easily recognizable in the topographic image of diatoms obtained in the constant-current mode. SECM in the constant-current mode is potentially a useful approach for topographic imaging of soft biological cells because it maintains the advantages of the constant-distance mode but eliminates the difficulties of a strong interaction force between the tip and sample.

## ACKNOWLEDGMENT

This work has been supported by grants from the National Science Foundation (CHE-9870762) and the Robert A. Welch Foundation. We acknowledge Drs. Yanbing Zu and Fu-Ren Fan for fruitful discussions and kind assistance in the experiments. Thanks also to Dr. David A. Vanden Bout for his generosity in allowing us to use his laser puller.

## SUPPORTING INFORMATION AVAILABLE

Resonance frequency and  $Q$ -factor of a 32.768-kHz tuning fork, resonance frequency (SI Table 1),  $Q$ -factor of a 100-kHz tuning fork (SI Table 2), schematic of SECM/OM setup (SI Figure 1), tip displacement in  $x$  and  $z$  direction (SI Figure 2), micrograph of *Navicula minima* (SI Figure 3), and tuning fork amplitude signal as a function of frequency for increasing immersion depths (SI Figure 4). This material is available free of charge via the Internet at <http://pubs.acs.org>

Received for review November 30, 2001. Accepted May 8, 2002.

AC015713U